Proppant Damage Characterization using Nuclear Magnetic Resonance Measurements*

Saurabh Tandon[1], Aderonke Aderibigbe[2], Zoya Heidari[1], Jingyu Shi[3], and Tihana Fuss-Dezelic[3]

Search and Discovery Article #80552 (2016)**
Posted November 7, 2016

*Adapted from extended abstract in relation to poster presentation given at AAPG 2016 Annual Convention and Exhibition, Calgary, Alberta, Canada, June 16-22, 2016.

[1]Department of Petroleum and Geosystems Engineering, The University of Texas at Austin, Austin, TX (zoya@utexas.edu)
[2]Department of Petroleum Engineering, Texas A&M University, College Station, TX
[3]Saint-Gobain Proppants, Stow, OH

Abstract

Proppant performance can significantly affect production in unconventional plays. Quantifying the mechanical damage and conductivity of proppants are, however, challenging. This paper introduces a new method using Nuclear Magnetic Resonance (NMR) measurements to characterize pore-size distribution in proppant packs. Pore-size distribution is affected by mechanical damage and conductivity of proppant packs and can be used to evaluate these properties. We carried out NMR measurements on proppant packs to quantify the sensitivity of NMR T_2 (spin-spin relaxation time)distribution to (a) different types of proppant with different surface relaxivity, (b) mixture of proppants with different sizes, and (c) proppants with different levels of mechanical damage.

The results show that NMR T_2 distribution is sensitive to pore-size distribution in the proppant packs which contain a mixture of proppants with different sizes and levels of mechanical damage. These measurements reflect the contribution of fines to the pore-size distribution of the proppant pack, and the effect of mechanical damage on different combinations of proppant size. We also observed measurable sensitivity of T_2 distribution to the different levels of mechanical damage in the proppant packs, which enabled quantifying damage in proppants. The loss of pore volume predicted by NMR T_2 distribution is in agreement with direct measurements applied on the proppant packs. Furthermore, we quantified the sensitivity of the NMR measurements to the proppants composed of different materials and coating. The results show that NMR T_2 distribution is sensitive to the presence of paramagnetic materials, such as iron in the proppants, especially if well distributed on the proppant surface. The results confirmed that the new method enables evaluating mechanical damage in proppant packs through quantifying pore structure in the packs, which eliminates the challenges with fluid-flow-based conventional techniques.

Introduction

The short- and long-term performance of proppants in hydraulic fracturing stimulation treatments depends on factors such as their size distribution, sphericity, and resistance to damage. These factors can influence the fracture conductivity, and hence the flow of hydrocarbons

from the reservoir to the wellbore. Proppant pack damage is in particular a major concern in fracture stimulation treatments. Both chemical and mechanical mechanisms can lead to proppant damage. Chemical mechanisms, such as proppant dissolution, fracturing fluid damage and geochemical reactions in the formation, result in changes in pore structure of the proppant packs (Weaver et al., 2010). Mechanical damage, from a combination of in situ stresses and temperature, results in proppant embedment, crushing, and fine generation, which cause a reduction in the porosity of the proppant pack. Hence, proppant damage characterization is important for the strategic selection of proppants for fracture treatment designs.

Previous publications have documented different approaches to analyze chemical and mechanical damages that cause loss of conductivity in proppant packs. Raysoni and Weaver (2012) analyzed macroscopic changes in proppant pack conductivity and used SEM images of proppants to illustrate the changes in pore structure due to the effect of proppant dissolution and subsequent remineralization. The API standardized crush test (API RP-19C, 2008) is commonly used in evaluating mechanical damage in proppants. However, the crush tests conditions do not adequately represent reservoir conditions, and crushing process is dependent on the type of proppant (Palisch et al., 2009; Getty and Balau, 2014). Aderibigbe et al. (2014) investigated and demonstrated the sensitivity of acoustic measurements to mechanical damage in proppant packs. Their studies also introduced the application of effective medium theories for the evaluation of effective elastic properties of the proppant packs and quantification of mechanical damage in proppant packs. The previous publications have focused on changes in macroscopic properties in the characterization of proppant pack damage. However, little attention has been given to pore-scale changes. Quantifying pore structure in proppant packs could improve the understanding of both mechanical damage and loss of conductivity.

NMR measurements have been extensively used in oil and gas industry for pore-scale characterization of rocks. NMR studies exploit the magnetic properties of hydrogen nuclei existing in the fluid present in the pore space by applying external magnetic field gradients (Torrey, 1956). At short echo spacing times, the transverse magnetization time of a pore fluid is a function of bulk relaxation of pore fluid, surface relaxation, and surface-to-volume ratio of the pores (Dunn et al., 2002; Brownstein and Tarr, 1977, 1979). T_2 distribution obtained from inversion of NMR signal can be used as a proxy of the pore-size distribution of the rock (Dunn et al., 2002).

In this article, we introduce a new NMR-based method for the characterization of pore-size distribution in proppant packs. We quantify the sensitivity of T_2 distribution to proppants of different types and sizes. Then, we damage the proppants to different levels by applying different uniaxial stress levels and quantified the sensitivity of T_2 distribution and geometric mean of T_2 distribution (T_{2gm}) to uniaxial stress applied and concentration of fines generated. The following sections describe the method for experiments, results and discussion, and conclusions of this study.

Method

Sample Preparation

We investigated three types of proppants with different compositions, sizes and surface properties. Table1 summarizes the properties of these proppants. Proppant Type C has magnetic coating, with surface properties different from the other two proppant types. A series of NMR experiments were carried out to quantify the NMR response in each of these proppants. We generated fines for use in the NMR experiments by

crushing these proppants. The proppant samples were placed in a cylindrical steel holder. The sample holder and piston assembly were placed in a loading frame where uniaxial stress of 22.5 MPa, 33.7 MPa, and 42.3 MPa were applied to the samples. The stress was applied at a constant displacement of 0.02 inches/min. After unloading the samples, the proppants were passed through standard sieve with mesh sizes 16 (1190 μm), 20 (840 μm), 30 (590 μm), 50 (300 μm), and 100 (150 μm), and stacked in a mechanical sieve shaker. The procedure applied for crushing the proppants is not the standard ISO procedure, but only specifically designed for generating fines. The term "fines" is used for any proppant size less than the size of original proppant obtained in the mixture after sieve analysis, while "proppant crush" is defined as proppants below 100 mesh size (150 μm). The sieved proppants were then used for NMR measurements.

NMR Experiments

The proppant packs used in NMR measurements were created by placing 10 g of proppants in small glass bottles. Water was added until it entirely covered the pack and excess water was drained. It was ensured that water displaces the air present in the pack. A benchtop 2MHz-frequency NMR spectrometer was used to measure T_2 distribution in the proppant packs. The NMR system used the Carr-Purcell-Meiboom-Gill (CPMG) pulse sequence for magnetic decay measurements (Torrey, 1956). The echo time of the sequence was kept at 80 microseconds. The minimum signal to noise ratio of 100 was used for acquisition of data. The data was calibrated to the total amount of water present in the sample. The least squares fitting method was then used for inversion for getting the T_2 distribution from the NMR magnetization decay. We carried out tests to investigate the sensitivity of the T_2 distribution measurements to (a) proppant composition, (b) combination e of proppant sizes, and (c) level of mechanical damage in the proppants packs.

Results and Discussion

Sensitivity of T_2 Distribution Measurements to Different Sizes and Compositions of Proppant

Figure 1 shows T_2 distribution obtained from 10 grams of different mesh sizes of proppant types A, B, and C. Table 2 summarizes the peaks of T_2 distributions obtained in Figure 1. Figures 1a and 1b show that T_2 peak decreases from 1232.2 ms to 613.59 ms (50.1% decrease) as proppant size decreases from 840 μm (20 mesh proppant) to 300 μm (50 mesh proppant) in proppant types A and B. The variation in T_2 distribution is more significant for proppant type C. Figure 1c shows that T_2 peak decreases from 813 ms to 305.39 ms (62.5 % decrease) as proppant size decreases from 840 μm (20 mesh proppant) to 300 μm (50 mesh proppant). The results confirmed that the size of the proppant grain controls the size of pores in the proppant pack and NMR can be effectively used for distinguishing among different proppant sizes. We also observe that the cumulative amount of fluids is almost the same in the different sizes of proppants in each proppant type A, B and C; this suggests that pore volume is almost the same in all the packs with different proppant sizes, pore-throat sizes, and pore-size distributions.

Figure 2 compares the T_2 distributions of the same size of proppants for different proppant types A, B, and C. T_2 distribution peak is almost the same for proppant types A and B and smaller in proppant type C in all the figures. The decrease in T_2 peak of proppant type C shows the influence of magnetic coating on the proppant.

Sensitivity of T_2 Distribution Measurements to Mixture of Proppants with Different Sizes

We analyzed the response of NMR on mixtures of different sizes of proppant type A. Figure 3 shows T_2 distribution in 20 mesh proppant mixed with 10% and 30% of 50 mesh proppant. Figure 3 also shows T_2 distribution in 20 mesh proppant mixed with 10% and 30% of "proppant crush." Figure 4 shows T_2 distribution in 30 mesh proppant mixed with 10% and 30% of 50 mesh proppant, and 10% and 30% of "proppant crush."

The results suggest that in the case of 20 mesh proppant, the cumulative water content decreases from 2.30 ml to 2.14 ml (7% decrease) as concentration of 50 mesh proppant increases from 0% to 30%. In the case of 30 mesh proppant, the cumulative water content decreases from 2.39 ml to 2.28 ml (4.6% decrease) as concentration of 50 mesh proppant increases from 0% to 30%. On the other hand, adding "proppant crush" significantly decreases the cumulative volume of water in the pack. In 20 mesh proppant, the cumulative water content decreases from 2.30 ml to 1.44 ml (37% decrease) when "proppant crush" concentration increases from 0% to 30%. In the case of 30 mesh proppant, the cumulative water content decreases from 2.39 ml to 1.51 ml (36% decrease) when "proppant crush" concentration increases from 0% to 30%

Geometric mean of T_2 distribution (T_{2gm}) can be used to quantify the variations in T_2 distribution of the mixtures. Figure 5a shows decrease in T_{2gm} with increase in percentage of 50 mesh proppant and "proppant crush" in 20 mesh proppant pack. T_{2gm} decreases from 900 ms to 532 ms when adding 50 mesh proppant but decreases from 900 ms to 122 ms when "proppant crush" is added. Similarly, Figure 5b shows decrease in T_{2gm} with increase in percentage of 50 mesh proppant and "proppant crush" in 30 mesh proppant pack. T_{2gm} decreases from 600 ms to 416 ms when adding 50 mesh proppant and decreases from 600 ms to 144 ms when "proppant crush" is added. It can be inferred from the results that T_{2gm} is more significantly decreased in the presence of "proppant crush."

Sensitivity of T_2 Distribution Measurements to Proppants Undergone Different Levels of Mechanical Damage

Proppant type A is damaged by three levels of uniaxial stress of 22.5 MPa, 33.7 MPa and 42.3 MPa. Figure 6 shows the stress-strain response of the 30 mesh proppant type A, when subjected to uniaxial stress of 42.3 MPa. It is observed that at stress of about 43 MPa, the proppant is still in the elastic regime.

Figure 7a shows the weight fraction of fines generated when applied stress reaches 42.3 MPa for both 20 mesh proppant and 30 mesh proppant. The weight fraction of fines generated in the case of 20 mesh proppant increases to 0.3 and in the case of 30 mesh proppant increases to 0.18 as applied stress increases to 42.3 MPa. Figure 7b illustrates the variation in T_{2gm} as weight fraction of fines generated for both 20 and 30 mesh proppant increases. In the case of 20 mesh proppant, T_{2gm} decreases from 900 ms to 650 ms (28% decrease) as fines concentration increases from 0% to 30%, and for 30 mesh proppant, T_{2gm} decreases from 600 ms to 530 ms (12% decrease) as fines concentration increases from 0% to 30%. The results suggest that the decrease in T_{2gm} is directly correlated to weight fraction of fines generated and mechanical damage to the proppant pack. It should be noted that the proppants used in the experiments are still within their elastic regime. The trend of fines generation might change when the proppant pack approaches the limit of elastic regime.

Conclusions

This article introduces the application of NMR measurements for characterization of pore-size distribution and quantification of mechanical damage in proppant packs. The results confirmed that changes in T_2 distribution can be easily correlated to changes in pore structure of proppant packs, either by quantifying the location of T_2 peaks or by calculating T_{2gm}. NMR T_2 distributions in proppant mixtures with different grain sizes and concentrations of crushed proppants show that NMR measurements are sensitive to the presence of smaller particles and crushed proppants. For instance, T_{2gm} decreased by up to 86% due to deposition of "proppant crush" in one of the proppant packs. Mechanical damage in the proppant packs decreased T_{2gm} by up to 28%, which was correlated to the increase in concentration of fines in the proppant pack. The results also confirmed that the NMR response is sensitive to both the size and coating of proppants. For instance, presence of magnetic coating decreased the T_2 peak by up to 62.5%.

The results are promising for application of the introduced method for evaluating mechanical damage and conductivity in proppant packs through quantifying pore structure in the packs. This new NMR-based method eliminates the challenges with fluid-flow-based conventional techniques. Furthermore, the results are promising for application of this characterization technique for in situ assessment of proppant conductivity. Finally, the introduced technique can be used to define required criteria for strategic selection of proppants in stimulation design, which is a requirement for successful development of unconventional plays.

Acknowledgements

Special gratitude goes to Saint-Gobain Proppants for providing proppant samples, crushing cylinder assembly used in laboratory experiments, and the permission for publishing this paper.

List of Acronyms

API	American Petroleum Institute
CPMG	Carr Purcell Meiboom Gill
NMR	Nuclear Magnetic Resonance

Selected References

Aderibigbe, A., C.C. Valdes, Z. Heidari, and T. Fuss, 2014, Mechanical damage characterization in proppant packs using acoustic measurements (presented at International Petroleum Technology Conference): IPTC-18092-MS.

API RP 19C, Recommended Practices for Measurement of Properties of Proppants Used in Hydraulic Fracturing and Gravel-Packing Operations, 2008, Washington, DC: American Petroleum Institute.

Brownstein, K.R., and C.E. Tarr, 1977, Spin-lattice relaxation in a system governed by diffusion: Journal of Magnetic Resonance, v. 26/1, p. 17-24.

Brownstein, K.R., and C.E. Tarr, 1979, Importance of classical diffusion in NMR studies of water in biological cells: Physical Review A, v. 19/6.

Coates, G.R, L. Xiao, and M.G. Prammer, 1999, NMR Logging Principals and Applications: Halliburton Energy Services, Houston, p. 65-69.

Dunn, K.J., D.J. Bergman, and G.A. Latorraca, 2002, Nuclear Magnetic Resonance Petrophysical and Logging Applications: Oxford, Elsevier Science Ltd, p. 71-101.

Freeman, D.A., J.J. Renkes, and D. Milton-Tayler, 2006, Qualifying proppant performance. (presented at SPE Annual Technical Conference and Exhibition): SPE 103623.

Getty, J., and C.R. Bulau, 2014, Are the laboratory measurements of proppant crush resistance unrealistically low? (presented at the Unconventional Resources Conference): SPE 168975.

Palisch, T.T., R. Duenckel, and M.A. Chapman, 2010, How to use and misuse proppant crush tests: Exposing the top 10 myths (presented at the Hydraulic Fracturing Technology Conference): SPE 168975.

Raysoni, N., and J.D. Weaver, 2012, Long-term proppant performance (presented at International Symposium and Exhibition on Formation Damage Control): SPE 150669.

Torrey, H.C., 1956, Bloch equations with diffusion terms: Physical Review, v. 104/3.

Weaver, J., R. Rickman, H. Luo, and R. Loghry, 2009, A study of proppant-formation reactions (presented at SPE International Symposium on Oilfield Chemistry): SPE 121465.

Proppant Type	Size (Mesh)	Size (μm)	Roundness	Sphericity
A	20, 30, 50	840, 590, 300	0.9	0.9
B	20, 30, 50	840, 590, 300	0.9	0.9
C	20, 30, 50	840, 595, 300	0.9	0.9

Figure 1. NMR T_2 distribution in the cases of (a) proppant type A, (b) proppant type B, and (c) proppant type C for 20-, 30-, and 50-mesh proppants. The solid and dotted lines show incremental and cumulative volumes, respectively.

Sieve Mesh Size	Proppant Type		
	A	B	C
20	1232.9	1232.9	811.1
30	811.13	705.5	533.6
50	613.6	613.6	305.4

Figure 2. NMR T_2 distribution in the cases of (a) 20 mesh proppant, (b) 30 mesh proppant, and (c) 50 mesh proppant. The solid and dotted lines show incremental and cumulative volumes, respectively.

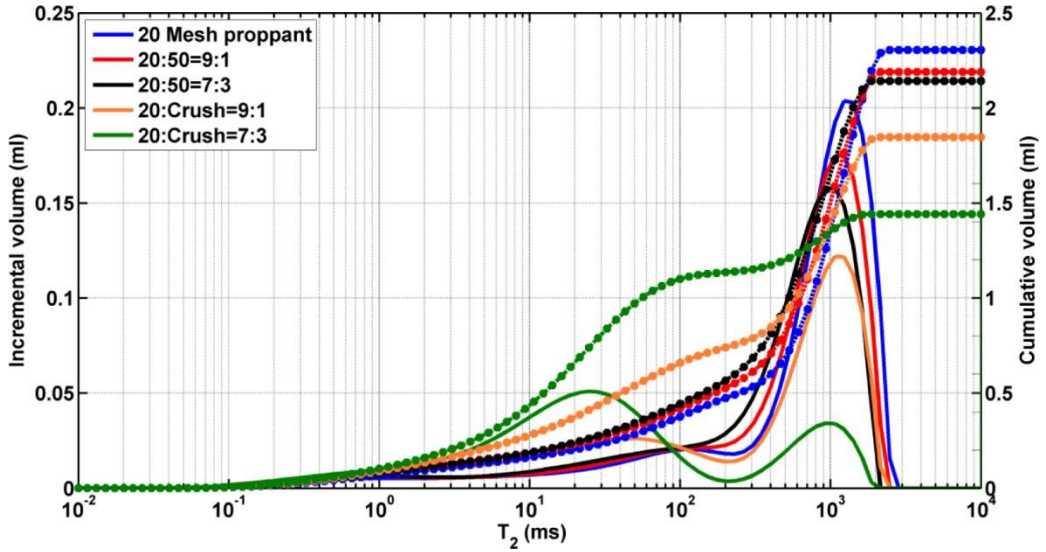

Figure 3. NMR T_2 distribution in the case of mixtures of 20 mesh proppant of type A with 50 mesh proppant and "proppant crush." The solid and dotted lines show incremental and cumulative volumes, respectively.

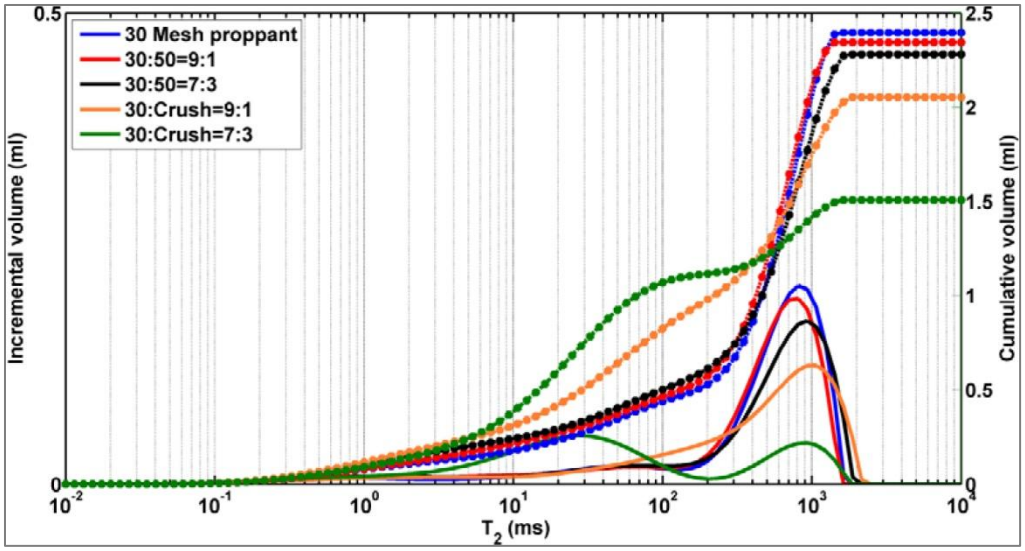

Figure 4. NMR T_2 distribution in the case of mixtures of 30 mesh proppant of type A with 50 mesh proppant and "proppant crush." The solid and dotted lines show incremental and cumulative volumes, respectively.

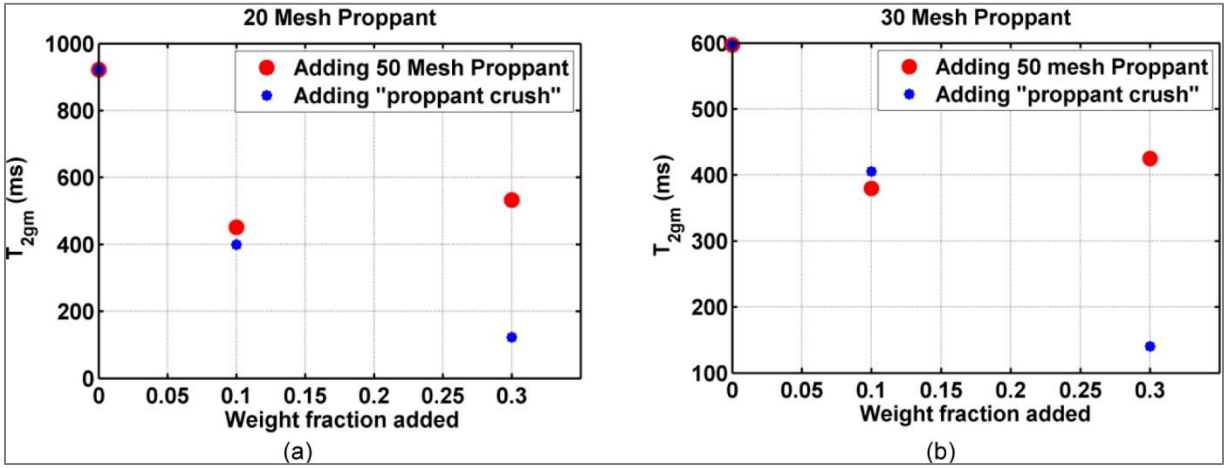

Figure 5. Variation of T_{2gm} after adding (a) 50 mesh proppant and "proppant crush" to the 20 mesh proppant pack and (b) 50 mesh proppant and "proppant crush" to 30 mesh proppant pack.

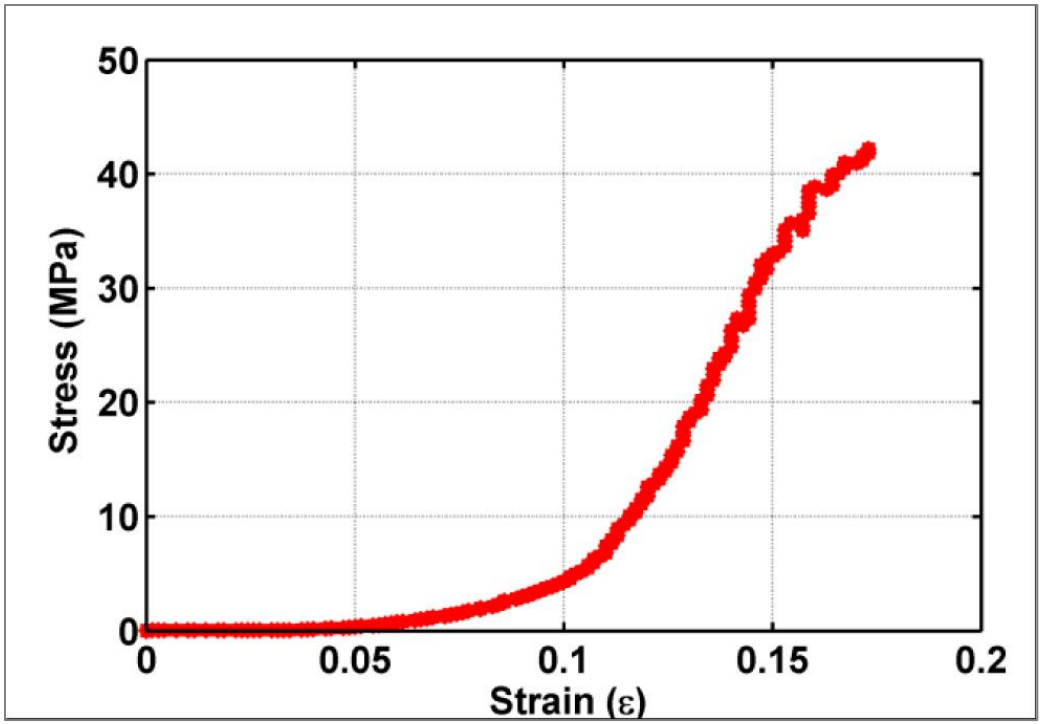

Figure 6. Proppant type A: Stress-strain correlation in the case of 30 mesh proppant.

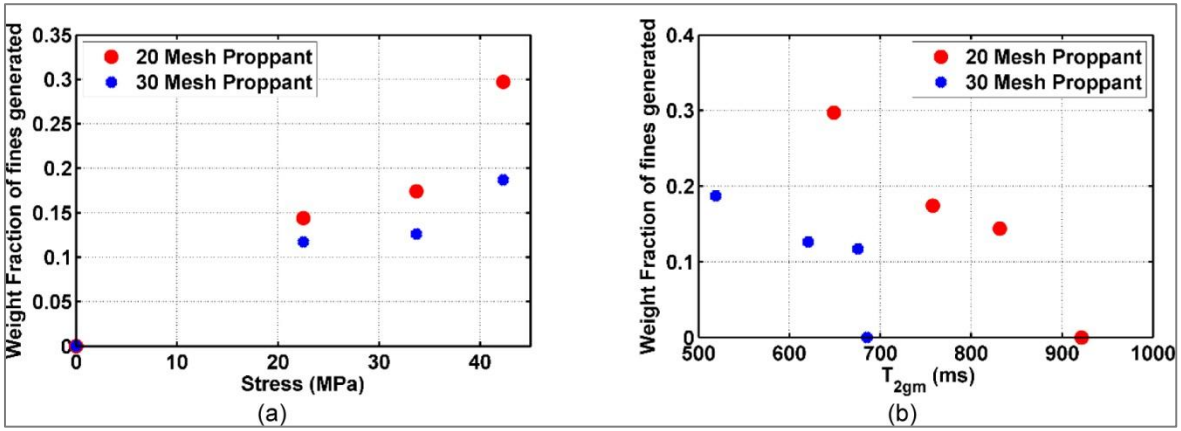

Figure 7. Impact of mechanical damage on weight fraction fines generated and NMR T_{2gm}: (a) Impact of increase in applied uniaxial stress on weight concentration of fines generated and (b) impact of weight concentration of fines generated on NMR T_{2gm}.

Proppant Type	Size (Mesh)	Size (μm)	Roundness	Sphericity
A	20, 30, 50	840, 590, 300	0.9	0.9
B	20, 30, 50	840, 590, 300	0.9	0.9
C	20, 30, 50	840, 595, 300	0.9	0.9

Table 1. Properties of proppants used for NMR testing.

Sieve Mesh Size	Proppant Type		
	A	B	C
20	1232.9	1232.9	811.1
30	811.13	705.5	533.6
50	613.6	613.6	305.4

Table 2. T_2 distribution peaks (in ms) for proppant types A, B, and C and proppant sizes of 850 μm (20 mesh proppant), 600 μm (30 mesh proppant), and 300 μm (50 mesh proppant).